



HHS Public Access

Author manuscript

J Biomed Mater Res B Appl Biomater. Author manuscript; available in PMC 2020 July 05.

Published in final edited form as:

J Biomed Mater Res B Appl Biomater. 2019 April ; 107(3): 479–489. doi:10.1002/jbm.b.34138.

***In vivo* biocompatibility and time-dependent changes in mechanical properties of woven collagen meshes: A comparison to xenograft and synthetic mid-urethral sling materials**

Katherine Chapin^{1,*}, Ahmad Khalifa^{2,3,*}, Thomas Mbimba⁴, Phillip McClellan⁴, James Anderson^{1,5}, Yuri Novitsky⁶, Adonis Hijaz³, Ozan Akkus^{1,4,7}

¹Department of Biomedical Engineering, Case Western Reserve University, Cleveland, Ohio 44106

²Faculty of Medicine in Urology, Menoufia University, Shebeen El-Kom, Egypt

³Department of Urology, University Hospitals Cleveland Medical Center, Cleveland, Ohio 44106

⁴Department of Mechanical and Aerospace Engineering, Case Western Reserve University, Cleveland, Ohio 44106

⁵Department of Pathology, Case Western Reserve University, Cleveland, Ohio 44106

⁶Department of General Surgery, University Hospitals Cleveland Medical Center, Cleveland, Ohio 44106

⁷Department of Orthopaedics, Case Western Reserve University, Cleveland, Ohio 44106

Abstract

Meshes woven from highly aligned collagen threads crosslinked using either genipin or 1-ethyl-3-(3-dimethylaminopropyl) carbodiimide and *N*-hydroxy succinimide (EDC/NHS) were implanted in a subcutaneous rat model to evaluate their biocompatibility (at 2 weeks, 2 months, and 5 months), mechanical properties (at baseline, 2 months, and 5 months) and ultimately their suitability for use as mid-urethral slings (MUS) for management of stress urinary incontinence. Porcine dermal (Xenmatrix) and monofilament polypropylene (Prolene) meshes were also implanted to provide comparison to clinically used materials. Quantitative histological scoring showed tissue integration in Xenmatrix was almost absent, while the open network of woven collagen and Prolene meshes allowed for cellular and tissue integration. However, strength and stiffness of genipin-crosslinked collagen (GCC), Prolene, and Xenmatrix meshes were not significantly different from those of native rectus fascia and vaginal tissues of animals at 5 months. EDC/NHS-crosslinked collagen (ECC) meshes were degraded so extensively at five months that samples could only be used for histological staining. Picrosirius red and Masson's trichrome staining revealed that integrated tissue within GCC meshes was more aligned ($p = 0.02$) and appeared more concentrated than ECC meshes at 5 months. Furthermore, immunohistochemical staining showed that GCC meshes attracted a greater number of cells expressing markers for M2 macrophages, those associated with regeneration, than ECC meshes ($p = 0.01$ for CD206+ cells, p

Correspondence to: O. Akkus; oxa@case.edu.

*Both authors contributed equally to this work.

= 0.001 CD163+ cells) at 5 months. As such, GCC meshes hold promise as a new MUS biomaterial based on favorable induction of fibrous tissue resulting in mechanical stiffness matching that of native tissue.

Keywords

stress urinary incontinence; collagen; tissue engineering

INTRODUCTION

Stress urinary incontinence (SUI) is the involuntary leakage of urine upon exertion or effort. SUI is a major urological healthcare problem that has been estimated to affect anywhere from 3 to 17% of women in the US.¹ Placement of a mid-urethral sling (MUS) is a common method for surgical management of SUI. Put very simply, the ideal material for a MUS would be biocompatible, readily manufactured, and able to provide support throughout the patient's lifetime. Several materials have been used as MUS over the years, but none have yet met the standards of an ideal material.

Autologous graft materials were popular for use as MUS because of their ability to promote host tissue integration and remodeling of the sling material into durable, long-term support for the urethra. However, additional procedures to harvest graft tissue have been found to result in morbidity at the donor site in addition to increasing post-operative pain and prolonging hospital stays.² Decellularized porcine dermis had been explored as a biomaterial alternative for SUI management, but unfavorable clinical outcomes due to poor tissue integration or insufficient crosslinking resulting in premature degradation of the material have limited their use.³

Synthetic mesh materials, mono-filamentous polypropylene (PP) specifically, have become the gold standard MUS material following success in several long-term studies.^{4,5} The non-degradable nature and ability to promote tissue integration due to their macroporous, monofilament design allow these meshes to provide stable support for the lifetime of patients. However, erosion and extrusion - the rubbing into and wearing through vaginal tissue respectively-are two painful and high-profile complications associated with PP MUS. Both are hypothesized to be the result of a mis-match in mechanical properties between the material and native tissue.⁶ Incidence of these complications following PP MUS placement for SUI management have been reported to range from 0 to 4.8%.⁷ Regardless these complications are remain so impactful to patients that they have led to FDA warnings and re-evaluation of the use of PP meshes as MUS by the medical community.⁸

There is still a need for the ideal MUS material. A material which integrates with host tissue and provides lifetime support like PP meshes, but interacts with tissues like autologous mesh materials- which have an extremely low incidence of erosion and extrusion- is the goal.⁹ Our group has developed a method for producing pure, woven collagen meshes which we believe fill the needs of the ideal MUS material. We have demonstrated that the mechanical properties of these meshes are robust and can be tailored based on their intended use. We have also demonstrated that they are capable of supporting cellularization *in vitro*.¹⁰

The purpose of the current study was two-fold. First, to determine the potential of woven collagen meshes to be used as MUS by evaluating their biocompatibility and mechanical properties alongside PP and xenograft MUS materials in a subcutaneous rat model. PP and xenograft meshes were used for comparison given their respective successes and failures in meeting the standards of an ideal MUS material. The second purpose of this study was to determine whether the type of crosslinking agent used to prepare woven collagen meshes would significantly affect their biocompatibility and biomechanics.

MATERIALS AND METHODS

Fabrication of woven collagen meshes

Electrochemically aligned collagen (ELAC) threads, made as previously described, were crosslinked and woven into meshes.¹⁰ ELAC threads were crosslinked using genipin or using a combination of 1-ethyl-3-(3-dimethylaminopropyl) carbodiimide and *N*-hydroxy succinimide (EDC/NHS) prior to weaving. Briefly, genipin crosslinking was done using a solution of 2% genipin in 70% ethanol/water for three days at 37°C. Threads were rinsed extensively in 1XPBS before being twisted into two-ply yarns. EDC/NHS crosslinking was done using a 67 mM EDC/167 mM NHS solution in 80% ethanol/water. Threads were crosslinked in solution for two hours at room temperature. The crosslinking solution was refreshed after two hours, and a second round of crosslinking was performed for an additional half hour at room temperature. Threads were then rinsed extensively in 1X PBS before being twisted into two-ply yarns [Figure 1(A,B)].

The two-ply genipin crosslinked collagen (GCC) yarns and EDC/NHS crosslinked collagen (ECC) yarns were woven into 10 × 10 mm squares for evaluating biocompatibility, or 5 × 20 mm rectangles for mechanical testing. Weaving was done by winding yarns in a zig-zag pattern through an array of 1 mm diameter pins set equidistant (0.5 mm) in a solid base of plastic. Once meshes were woven to the desired size on the pins, a 10% PLGA solution was added to remove the mesh from the pins. Another yarn was then woven through the spaces left by the pins to secure the mesh together. Finally, meshes were briefly submerged in chloroform to remove the PLGA coating before being thoroughly rinsed in 1XPBS. This method has been previously documented by our group¹⁰.

Prolene (Ethicon, New Jersey), a monofilament polypropylene mesh, and Xenomatrix (Davol Inc., Rhode Island), a decellularized porcine dermal matrix, were chosen as the synthetic and xenograft controls respectively. Meshes for biocompatibility and mechanical testing were cut to the same size as their collagen mesh counterparts [Figure 1(C-J)].

Subcutaneous implantation of woven collagen meshes

All animal procedures were performed in accordance with rules and protocols approved and established by the Institutional Animal Care and Use Committee (IACUC) at Case Western Reserve University. Animals were anesthetized using a mixture of ketamine and xylazine administered via intraperitoneal injection. Prior to surgery, all meshes were sterilized in a 0.1% peracetic acid (PAA) ethanol solution and rinsed thoroughly with sterile PBS.

To place meshes for biocompatibility testing under the abdominal skin two 1 cm midline incisions were made, one below the sternum and the other above the symphysis pubis. To place meshes for mechanical testing under the dorsal skin two 2 cm midline incisions were made, one below the cervical spine and the other 1.5 cm above the tail. Bilateral tunneling was used to open space on either side of incisions, creating four subcutaneous spaces for meshes to be placed.

A total of 25 animals were used in this study; 15 were used exclusively for evaluating biocompatibility of meshes and 10 were used exclusively for evaluating the mechanical properties of meshes. Each of the 15 animals used exclusively for evaluating biocompatibility of meshes had four total meshes implanted subcutaneously in its abdomen, one each of Xenmatrix, Prolene, GCC, and ECC. Five animals were sacrificed at each time point of 2 weeks, 2 months, and 5 months. Samples were harvested from the abdomen by collecting the skin and underlying abdominal muscle tissue along with mesh materials. Time points for harvest were chosen to align with significant time points in the healing response to implanted materials.¹¹ Each of the 10 animals used exclusively for evaluating mechanical properties of meshes had four total meshes implanted subcutaneously in the dorsal region. Five animals each were sacrificed at 2 and 5 months. Samples were dissected from the overlying skin and underlying muscle layers such that integrated tissue was not disturbed. Time points for harvest and testing were chosen to align with those used for biocompatibility testing, with the exception of the 2-week time point, as the mechanical properties of meshes were assumed to not be significantly different from baseline after reviewing results from similar studies in literature.^{12,13} Freshly prepared meshes were tested and used for baseline measurement.

Histological staining and scoring for host response and tissue integration

Explanted mesh samples were fixed in 10% formalin for five days and dehydrated before being embedded in paraffin, cut into 5 µm thick sections and mounted onto slides. Slides were stained using either hematoxylin and eosin (H&E), Masson's trichrome or picrosirius red (Polysciences, PA) using standard methods reported previously.^{10,14} H&E stained slides were scored by a senior pathologist (J. Anderson) in accordance with ISO 10993-6, "Biological Evaluation of Medical Devices- Part 6: Tests for Local Effects after Implantation."¹⁵ Slides were evaluated in a blinded fashion using a semi-quantitative scale rating from 0 to 4 for minimal to extensive presence of the following indicators of biocompatibility:¹⁵ acute inflammation, chronic inflammation, granulation tissue, foreign body response, fibrous encapsulation, neovascularization, cellular infiltration, new collagen deposition and fibroblast proliferation. Measures of host response- granulation tissue, foreign body response and fibrous encapsulation- were scored at the perimeter of mesh materials (Table I, Figures 2–3). Measures of tissue integration and cellular infiltration - neovascularization, cellular infiltration, new collagen deposition and fibroblast proliferation- were scored within the perimeter of mesh materials (Table II, Figures 2–3).

Mechanical testing

Samples were tested immediately after sacrifice and harvest. Groups of "baseline" (freshly prepared) meshes ($n = 5$ per mesh type) as well as freshly harvested rectus fascia and vaginal

tissue ($n = 5$ of each) were also tested. All samples were pre-wet in 1XPBS before testing. Samples were fixed between grips and subjected to uniaxial tensile loading until failure at a rate of 10 mm/min using a universal testing machine (Test Resources, Minnesota). Load and displacement data were recorded and used along with sample width and thickness to calculate stress and modulus values (Table III and Figure 4).

Immunohistochemical staining for woven collagen meshes

Immunohistochemical staining was performed on woven collagen mesh samples to further explore differences in outcomes for host response related to the two crosslinking methods. Dehydrated and mounted samples were prepared in the same manner as those for histological staining.¹⁰ The following antibodies were used to identify macrophages; general macrophage population: anti-CD68 (Abcam, Massachusetts), M1—anti-B7 (Santa Cruz, TX, Dallas) and IL-6 (Santa Cruz), M2—anti-CD163, anti-CD206 (Santa Cruz). Anti-alpha smooth muscle and anti-CD31 (Abcam) were chosen as markers for endothelium cells to evaluate tissue vascularization. Sections were incubated with alkaline phosphatase-conjugated secondary antibodies (Abcam), after which staining was developed using the alkaline phosphate substrate-chromogen StayRed/AP kit (Abcam). Slides were imaged using the Olympus IX83 microscope and CellSens software (Olympus). The number of stained, expressive cells within a high-powered, 40X magnification, field (HPF) were counted and reported. Three fields were taken per section, and five sections were evaluated per explanted mesh type, for a total of 15 measurements per mesh type per time point (Figures (5 and 6)).

Changes in thread area density and cross-sectional area of woven collagen meshes

The thread area density (percentage of the total woven collagen mesh areas occupied by ELAC threads) and cross-sectional area of woven collagen meshes were measured using images of H&E stained samples. Images and measurements were acquired at 5X magnification using an Olympus IX83 microscope, the accompanying CellSens software (Olympus, Pennsylvania) and ImageJ (National Institute of Health, Bethesda, Maryland). One section per explanted mesh per time point was evaluated, for a total of 5 measurements taken for ECC and GCC meshes at each time points (Figure 7).

Alignment of newly deposited collagen

The alignment of newly deposited collagen in woven collagen meshes was evaluated by measuring the average corrected pixel intensity of images of picrosirius red stained samples obtained at 10X magnification under cross polarized light using ImageJ (National Institute of Health).^{16,17} Three images were taken per section and, five sections were evaluated per explanted mesh for a total of 15 measurements per mesh type per time point (Figure 8)

Statistical analysis

The non-parametric Kruskal Wallis test was used for overall comparison of mechanical testing groups, while the Mann Whitney *U* test was used to make *post hoc* pair-wise comparisons. The Mann Whitney test was also used to examine pairwise significant differences between quantitative histology measures and scores. All pairwise comparisons

were made using the Bonferroni correction. All tests were performed at $\alpha = 0.05$ in R (University of Auckland, New Zealand).

RESULTS

Scoring for host response and tissue integration

All meshes were able to be recovered for histological testing at 5 months, although ECC meshes appeared to be degraded to a more significant degree. One ECC mesh explanted at 2 weeks was given a score of 1 for acute inflammation, and one explanted at 2 months was given a score of 1 for chronic inflammation. These low scores in a limited number of samples are not indicative of toxicity. All remaining meshes were given scores of zero for both acute and chronic inflammation at all time points.

At 5 months there were no significant difference in scores for new collagen deposition between GCC and ECC meshes ($p = 0.3$) or between GCC and Prolene meshes ($p = 0.45$). These were the only comparisons made to conserve the level of significance in testing.

Mechanical testing

GCC meshes had significantly greater moduli and stress to failure than native tissues at baseline (modulus, $p = 0.004$ for both, stress to failure, $p = 0.012$ for both) [Figure 4(A,B), Table III]. The strength and stiffness of GCC meshes at 5 months was comparable to those of native tissues ($p > 0.05$).

Modulus and stress to failure values for ECC meshes were greater than native tissues at the baseline ($p = 0.012$ for both), and significantly less at 2 months ($p = 0.022$ for both). Although ECC meshes were recovered for histological and immunohistochemical staining at five months, none were able to be recovered and used for mechanical testing. Samples were degraded or integrated with surrounding tissue to the extent that their size made testing infeasible [Table III, Figure 4(A–C)].

The moduli of Prolene meshes were significantly greater than native tissues at 2 months only (vaginal tissue, $p = 0.012$; rectus fascia, $p = 0.022$). Stress to failure for Prolene meshes was significantly greater than native tissues at baseline ($p = 0.012$ for both) and 2 months ($p = 0.012$ for both). At baseline and two months Xenmatrix meshes had significantly greater moduli (baseline, $p = 0.0012$ for both; two months, $p = 0.022$ for both) and stress to failure values (baseline, $p = 0.012$ for both; two months, $p = 0.012$ for both) than native tissues [Table III, Figure 4(A,B)].

Immunohistochemical staining for woven collagen meshes

At 2 months a significantly greater number of CD68+ cells were observed in ECC meshes than GCC meshes ($p = 0.002$). However, there was a significant decrease of observed CD68+ cells in ECC meshes between 2 and 5 months ($p = 0.001$), such that there was a significantly greater number observed in GCC meshes at 5 months ($p = 0.001$) [Figure 5(A)]. The same pattern was observed for IL-6+ cells [significances listed on Figure 5(C)]. There were no significant differences or changes in the number of observed B-7+ cells between or in either mesh type [Figure 5(B)]. A significantly greater number of CD163+

cells were observed in GCC meshes than ECC meshes at 2 and 5 months (2 months, $p = 0.01$; 5 months, $p = 0.01$) [Figure 5(D)]. The number of CD206+ cells in GCC meshes increased significantly over time ($p = 0.02$) and it was significantly greater than the number of CD206+ cells in ECC meshes at 5 months ($p = 0.001$) [Figure 5(E,F)].

The number of α -SMA+ cells decreased significantly from 2 to 5 months for both woven collagen meshes (genipin, $p = 0.001$; EDC/NHS, $p = 0.003$), but was significantly greater in GCC meshes than ECC meshes at 2 months ($p = 0.005$) [Figure 6(B)]. Finally, the number of CD31+ cells in ECC meshes decreased significantly between 2 and 5 months ($p = 0.001$), although there were no significant differences between GCC or ECC meshes at any time point [Figure 6(A)].

Changes in cross-sectional area and thread area density of woven collagen meshes

While there are limitations to these measurements- limited sample size and an inability to track mesh degradation longitudinally- the authors feel that the sections taken were representative of physical changes to meshes at those time points. GCC meshes had significantly greater cross-sectional area than ECC meshes at 2 weeks ($p = 0.015$) and 2 months ($p = 0.03$) [Figure 7(A)]. The cross-sectional area of GCC meshes did not change significantly over time [Figure 7(A)]. The thread area density of ELAC threads in GCC and ECC meshes decreased significantly between 2 weeks and 2 months ($p = 0.03$, genipin; $p = 0.03$, EDC/NHS), but neither decreased significantly between 2 and 5 months [Figure 7(B)].

Alignment of newly deposited collagen

The degree of alignment of newly deposited collagen within GCC meshes was significantly greater than that of ECC meshes at 2 months ($p = 0.007$) and 5 months ($p = 0.02$). There was no significant change in the degree of alignment of newly deposited collagen for ECC meshes, but there was a significant increase for GCC meshes from 2 to 5 months ($p = 0.004$) (Figure 8).

DISCUSSION

Comparing the results of GCC and ECC meshes to Prolene and Xenmatrix meshes can provide insight into their potential functionality as MUS. The higher scores for both groups of crosslinked collagen meshes for host response parameters granulation tissue and foreign body response over time might initially indicate they were eliciting a heightened response compared to Prolene and Xenmatrix (Table I). However, both granulation tissue- denoted by the presence of macrophages, blood vessels and fibroblasts- and the foreign body response are hallmarks of the normal healing response.¹¹ Also, densely woven fabrics such as the collagen meshes used in this study are known to incite an increased host response when compared to their smooth surface counterparts, like Prolene and Xenmatrix, given their increased surface to volume ratio.¹¹ Regardless, scores for collagen meshes in this study indicate they are biocompatible, similar to Xenmatrix and Prolene (Table I).

Fibrous encapsulation is mediated by the condition of the tissue framework surrounding an implanted material, and reflects the end stage of the normal healing response to that implanted material.¹¹ As such, it could be considered a measure of injury or persistence of

an implanted material as destruction of the surrounding tissue framework results in fibrosis. Increasing scores for Prolene were expected given the non-degradable nature of the mesh (Table I). Increasing scores for Xenmatrix were also expected, despite the fact that is not crosslinked, given previously reported results and the time points used in this study.^{16,17} Average fibrous encapsulation scores for GCC meshes were in the range of “moderate” to “extensive” (3.33 ± 0.58) whereas ECC meshes were given average scores of “mild” (2 ± 0) at 5 months (Table I). These results show that GCC meshes were persistent enough within the abdominal tissue framework to elicit moderate to extensive fibrous encapsulation over the time course of this study. These results also corroborate surgical observations from later time points as GCC meshes were recoverable while ECC meshes were not.

Scoring of tissue integration parameters provides further insight into the durability and longevity of meshes. While these parameters are certainly dependent on the porosity of a mesh’s design, as evidenced by poor integration scores for Xenmatrix, they are also heavily influenced by the constitution of the mesh materials themselves. This is especially evident in scoring for ECC meshes which displayed “extensive” cellular infiltration, but only received average scores of “minimal” to “mild” for new collagen deposition and fibroblast infiltration (1–2) over time. (Table I) These scores were also confirmed by Masson’s trichrome images [Figure 8(B)]. In contrast, scores for new collagen deposition and fibroblast proliferation increased with time for GCC meshes from the “moderate” to “extensive” (3–4) range [Table I, Figure 8(A)]. However, given the limited sample size of this study there were no significant differences between scores for new collagen deposition (Table I. These scores are still notable as they demonstrate that the design of the woven collagen meshes allowed for cellular infiltration (Table I).

Unlike biocompatibility, there are currently no established metrics in terms mechanical properties for MUS. Native vaginal tissue was used in this study as the mismatch in stiffness and strength between it and sling materials is hypothesized to increase the likelihood of erosion and extrusion either through direct injury or due to atrophy of the vaginal tissue through a stress shielding like mechanism.^{9,18,19} Native rectus fascia was also used given the success of autograft slings in managing incontinence with a lack of erosions.⁴

The load bearing mechanical properties of Prolene meshes increased from baseline to 2 months, but then decreased from 2 to 5 months [Figure 4(A,B)]. Previous studies report a continued increase, or eventual plateau of load bearing properties with continued tissue integration adding stiffness and strength to the mesh.¹² Although there was no significant difference between the modulus or stress to failure of Prolene meshes and native tissues at 5 months, the values for Prolene meshes were still at least two times higher than those of native tissues [Figure 4(A,B)].

The goal for a biological mesh to be used as MUS is to elicit ingrowth of fibrous tissue concurrent with degradation of the mesh such that the decline of the mechanical properties halts as the mesh is completely replaced by host tissue. The declining load bearing properties of Xenmatrix meshes indicate that limited porosity of meshes restricted tissue, or even cellular, infiltration and resulted in degradation of the meshes within the fibrous capsule. In contrast the structure of ECC meshes allowed for infiltration by host cells, but

the material itself was not durable enough to resist degradation and elicit tissue development and integration. Unlike either Xenmatrix or ECC meshes, the modulus of GCC meshes were maintained by later time points as their porosity and durability allowed for tissue integration that supported the remaining mesh material [Figure 4(A,B)]. These results are particularly important as they represent the functional outcome of the differences in, and highlight the importance of, tissue integration for the woven collagen meshes in this study.

Immunostaining results were used further to investigate the differences in host response between the two different crosslinking moieties. In general, GCC meshes had a higher degree of immunostaining for expression of anti-inflammatory markers (CD163, CD206) and lower degree of pro-inflammatory markers (B7, IL-6) than ECC meshes [Figure 5(B-E)]. Although there was a significant increase in the number of IL-6+ cells from 2 to 5 months for GCC meshes, there was also a significant increase in the number of CD206+ cells and no significant change in the number of CD163+ cells. This may show a shift in the innate immune response from pro-inflammatory to anti-inflammatory in GCC meshes between 2 and 5 months. Genipin is derived from the gardenia fruit which has historically been used in herbal remedies for inflammation. Recent studies have confirmed that genipin acts as an anti-inflammatory agent and may promote expression of anti-inflammatory markers in macrophages.²⁰ Thus, increased deposition of new, fibrous tissue in GCC compared to ECC meshes may have been driven by remodeling signals from genipin itself as evidenced by the continued expression of anti-inflammatory macrophages markers by cells within meshes over time.

Results of image analysis of H&E and picrosirius red staining of woven collagen meshes also illustrate differences in host response and tissue integration for the two crosslinking moieties. First, the thread area density and cross-sectional area of meshes in slides for both GCC and ECC meshes decreased from 2 weeks to 2 months, mirroring the results of mechanical testing and corroborating the fact that the initial decrease in stiffness is the result of degradation of the materials^{21,22}(Figure 7). Notably, and also mirroring the results of mechanical testing, the decreases were only significant for ECC meshes. Results of image analysis of meshes stained using picrosirius red were notable as they showed that GCC meshes had significantly higher degree of alignment of newly deposited collagen compared to ECC meshes at all time points [Figure 8(C)]. This is an important result as literature has shown that aligned tissue networks to be more mechanically robust than randomly aligned networks.²³

As the only difference between woven collagen meshes were the crosslinking regimens used to prepare them, it follows that the differences in the nature of these crosslinkers would give further insight into the results of the study. EDC/NHS is a zero-length crosslinker while genipin is an oligomeric crosslinker. EDC/NHS molecules can facilitate crosslinking between groups but do not become part of the bond. In contrast, genipin molecules become a permanent bridge between molecules as dimers or longer polymer chains. Several groups have shown that genipin molecules can polymerize into chains 30–40 molecules long before forming crosslinks.²⁴ The more extensive crosslinking regimen provided meshes with a degradation profile that allowed sufficient time for the later stages of the normal healing

response to an implanted material to develop. As noted earlier, the inherent anti-inflammatory properties of genipin may have contributed to the healing process as well.

There are limitations to this study that need to be addressed with further testing. First and foremost, meshes will need to be implanted and evaluated in the sub-urethral environment to fully determine their suitability in their intended application as MUS. The sub-urethral environment presents much different and greater challenges in terms of mechanical and biochemical stresses than the subcutaneous abdominal environment. The presence and efficacy of meshes will need to be evaluated at longer time points- 1 year and greater- than used in this study as well given that MUS must function for the lifetime of the patient. Further, a greater number of samples than used in this study will be needed to provide statistical power to findings and overcome testing limitations present in this study for quantitative histological scoring.

CONCLUSIONS

This study is a preliminary assessment of the feasibility of woven crosslinked collagen meshes to be used as MUS. Results showed EDC/NHS crosslinking regimen was not robust enough to prevent significant degradation beyond 2 months, or prior to fibrous tissue integration. The genipin crosslinking regimen not only provided meshes with a degradation profile long enough to develop through to the final stages of the normal healing response, but also may have aided that healing response with strong tissue remodeling signals. Although Prolene and other synthetics have demonstrated long term success there still exists a need for an alternative to synthetics for those patients who exhibit atrophied or weakened tissue for which synthetics may be contraindicated. While functional testing of genipin crosslinked meshes in the sub-urethral environment is necessary to confirm their appropriateness as an MUS material, results of subcutaneous implantation in this model demonstrate that these meshes are a promising candidate.

REFERENCES

1. Nitti VW. The prevalence of urinary incontinence. *Rev Urol* 2001; 3:2–6.
2. Sangster P, Roland M. Biomaterials in urinary incontinence and treatment of their complications. *Indian J Urol* 2010;26:221–229. [PubMed: 20877601]
3. Gandhi S, Kubba LM, Abramov Y, Botros SM, Goldberg RP, Victor TA, Sand PK. Histopathologic changes of porcine dermis xenografts for transvaginal suburethral slings. *Am J Obstet Gynecol* 2005;192:1643–1648. [PubMed: 15902171]
4. Khan ZA, Nambiar A, Morley R, Chapple CR, Emery SJ, Lucas MG. Long-term follow-up of a multicentre randomised controlled trial comparing tension-free vaginal tape, xenograft and autologous fascial slings for the treatment of stress urinary incontinence in women. *BJU Int* 2015;115:968–977. [PubMed: 24961647]
5. Nilsson C, Palva K, Aarnio R, Morcos E, Falconer C. Seventeen years' follow-up of the tension-free vaginal tape procedure for female stress urinary incontinence. *Int Urogynecol J* 2013;24: 1265–1269. [PubMed: 23563892]
6. Mangera A, Bullock A, Chapple C, Macneil S. Are biomechanical properties predictive of success of prosthesis used in stress urinary incontinence and pelvic organ prolapse? A systemic review. *Neurourol. Urodyn* 2012;31:13–21. [PubMed: 22038890]

7. Abouassaly R, Steinberg JR, Lemieux M, Marois C, Gilchrist LI, Bourque J-L, Tu LM, Corcos J. Complications of tension-free vaginal tape surgery: A multi-institutional review. *BJU Int* 2004;94: 110–113. [PubMed: 15217442]
8. Update on Serious Complications Associated with transvaginal placement of surgical mesh for POP. FDA Safety Communication; 2011 <<https://www.fda.gov/downloads/MedicalDevices/Safety/AlertsandNotices/UCM262760.pdf>>
9. Gigliobianco G, Regueros S, Osman N, Bissoli J, Bullock A, Chapple C, MacNeil S. Biomaterials for pelvic floor reconstructive surgery: How can we do better? *Biomed Res Int* 2015;2015:1–20.
10. Younesi M, Islam A, Kishore V, Anderson JM, Akkus O. Tenogenic induction of human MSCs by anisotropically aligned collagen biotextiles. *Adv Funct Mater* 2014;24:5762–5770. [PubMed: 25750610]
11. Anderson JM. Biological responses to materials. *Annu Rev Mater Res* 2001;31:81–110.
12. Dietz HP, Vancaillie P, Svehla M, Walsh W, Steensma AB, Vancaillie TG. Mechanical properties of urogynecologic implant materials. *Int Urogynecol J Pelvic Floor Dysfunct* 2003;14:239–243. [PubMed: 14530834]
13. Cannon TW, Sweeney DD, Conway DA, Kamo I, Yoshimura N, Sacks M, Chancellor MB. A tissue-engineered suburethral sling in an animal model of stress urinary incontinence. *BJU Int* 2005;96: 664–669. [PubMed: 16104928]
14. Noorlander ML, Melis P, Jonker A, Van Noorden CJF. A quantitative method to determine the orientation of collagen fibers in the dermis. *J Histochem Cytochem* 2002;50:1469–1474. [PubMed: 12417612]
15. ISO. Biological evaluation of medical devices- Part 6: Tests for local effects after implantation (Standard no. 10993–6). 2006 <https://www.iso.org/standard/61089.html>
16. Caetano GF, Fronza M, Leite M, Gomes A, Andrey M. Comparison of collagen content in skin wounds evaluated by biochemical assay and by computer-aided histomorphometric analysis. *Pharm Biol* 2016;54:2555–2559. [PubMed: 27180834]
17. Whittaker P, Kloner R, Boughner D, Pickering J. Quantitative assessment of myocardial collagen with picosirius red staining and circularly polarized light. *Basic Res Cardiol* 1994;89:397–410. [PubMed: 7535519]
18. Feola A, Abramowitch S, Jallah Z, Stein S, Barone W, Palcsey S, Moalli P. Deterioration in biomechanical properties of the vagina following implantation of a high-stiffness prolapse mesh. *BJOG Int J Obstet Gynaecol* 2013;120:224–232.
19. Feola A, Moalli P, Alperin M, Duerr R, Gandley RE, Abramowitch S. Active mechanics of the rat vagina. *Ann Biomed Eng* 2011;39: 549–558. [PubMed: 20824342]
20. Koo HJ, Lim KH, Jung HJ, Park EH. Anti-inflammatory evaluation of gardenia extract, geniposide and genipin. *J Ethnopharmacol* 2006;103:496–500. [PubMed: 16169698]
21. Annor AH, Tang ME, Pui CL, Ebersole GC, Frisella MM, Matthews BD, Deeken CR. Effect of enzymatic degradation on the mechanical properties of biological scaffold materials. *Surg Endosc* 2012; 26:2277–2275.
22. Macleod TM, Williams G, Sanders R, Green CJ. Histological evaluation of Permacol as a subcutaneous implant over a 20-week period in the rat model. *Br J Plast Surg* 2005;58:518–532. [PubMed: 15897038]
23. Leong B, Chan K. Scaffolding in tissue engineering: General approaches and tissue-specific considerations. *Eur Spine J* 2008; 17:467–479. [PubMed: 19005702]
24. Mu C, Zhang K, Lin W, Li D. Ring-opening polymerization of genipin and its long-range crosslinking effect on collagen hydrogel. *J Biomed Mater Res A* 2013;101:385–93. [PubMed: 22847997]

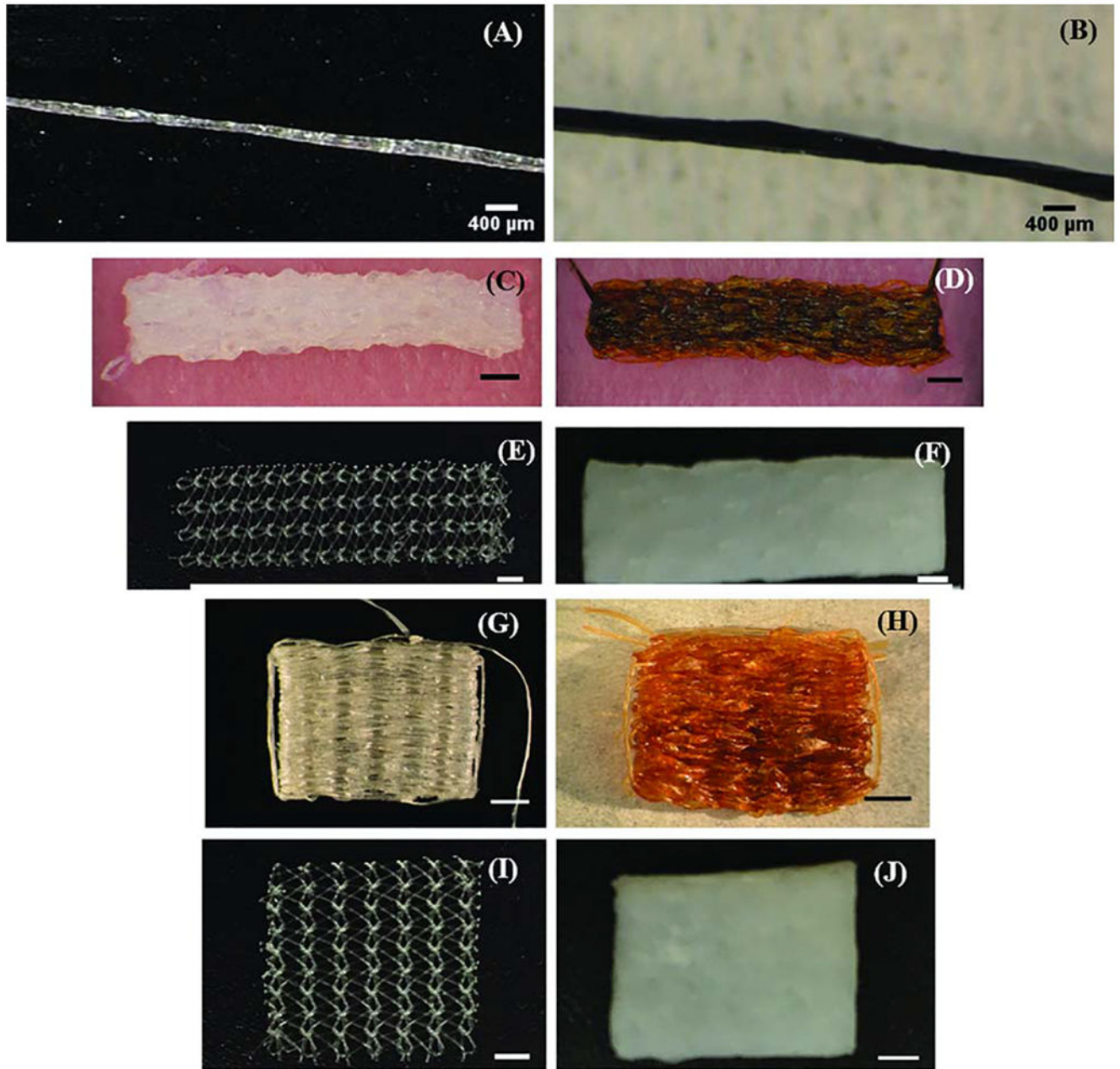


FIGURE 1.

Light microscopy images of (A) Two-ply ECC yarn (B) Two-ply GCC yarn (C–F) ECC, GCC, Prolene and Xenmatrix meshes implanted to evaluate mechanical properties (G–J) ECC, GCC, Prolene and Xenmatrix meshes for assessing mechanical properties. Scale bars for meshes are 2 mm.

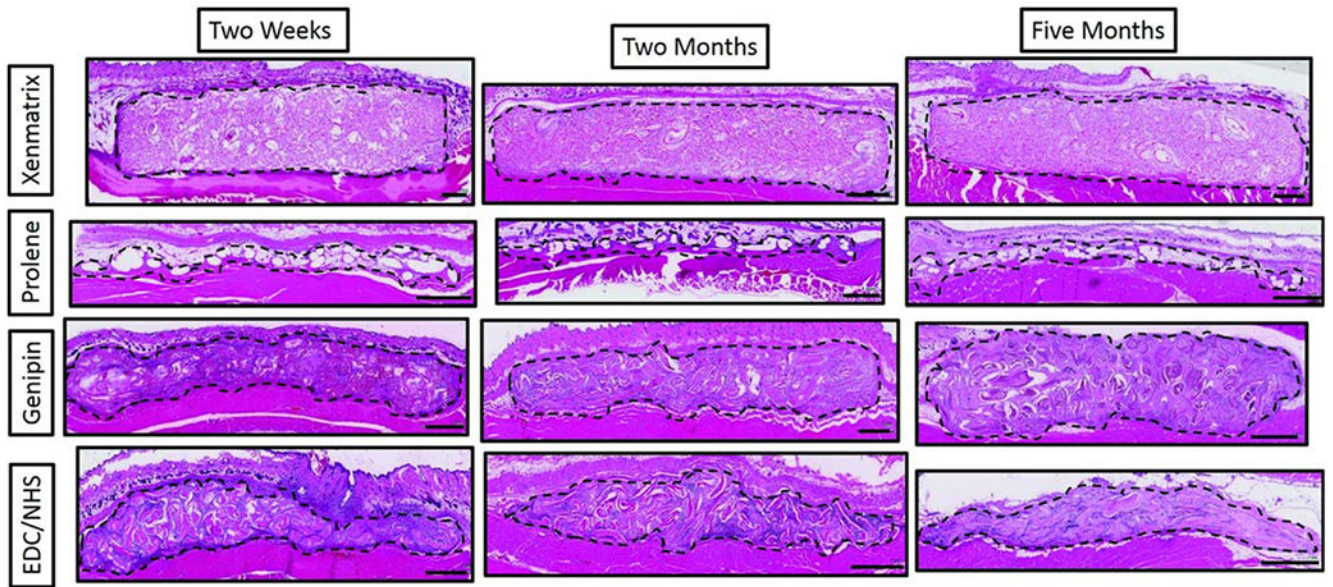


FIGURE 2.

Low magnification light microscopy images of H&E stained mesh sections at 2 weeks, 2 months and 5 months. Meshes were collected along with overlying skin and underlying abdominal muscle. Sections of meshes (within dotted outline) are oriented here with the skin at the top of images and the abdominal muscle at the bottom of the images. Scale bars are 1 mm.

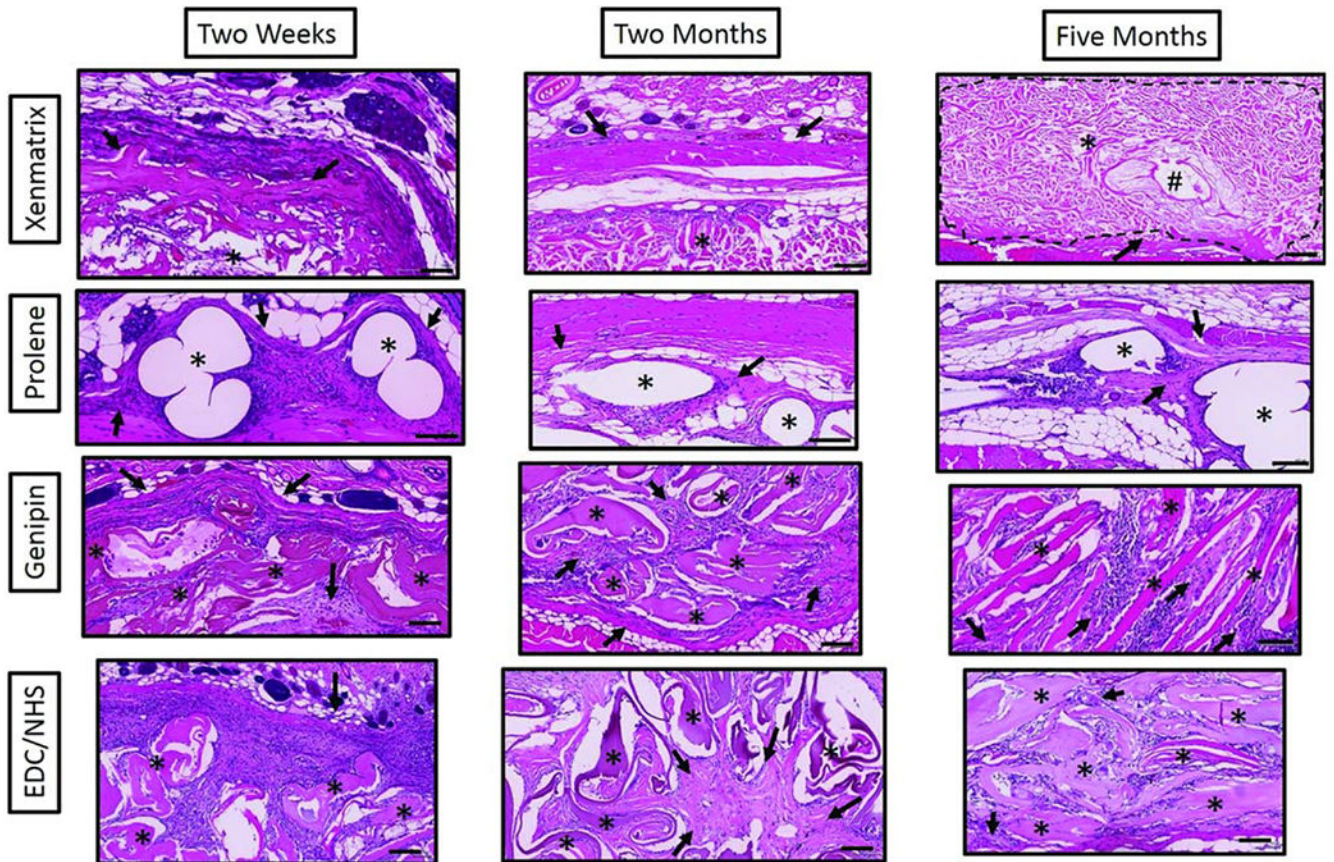


FIGURE 3.

High magnification light microscopy images of H&E stained mesh sections at 2 weeks, 2 months and 5 months. Stars denote the respective mesh materials and arrows indicate areas of new collagen deposition in an around mesh materials. The pound symbol (#) denotes hair follicles in Xenmatrix mesh sections. Scale bars are 100 μm .

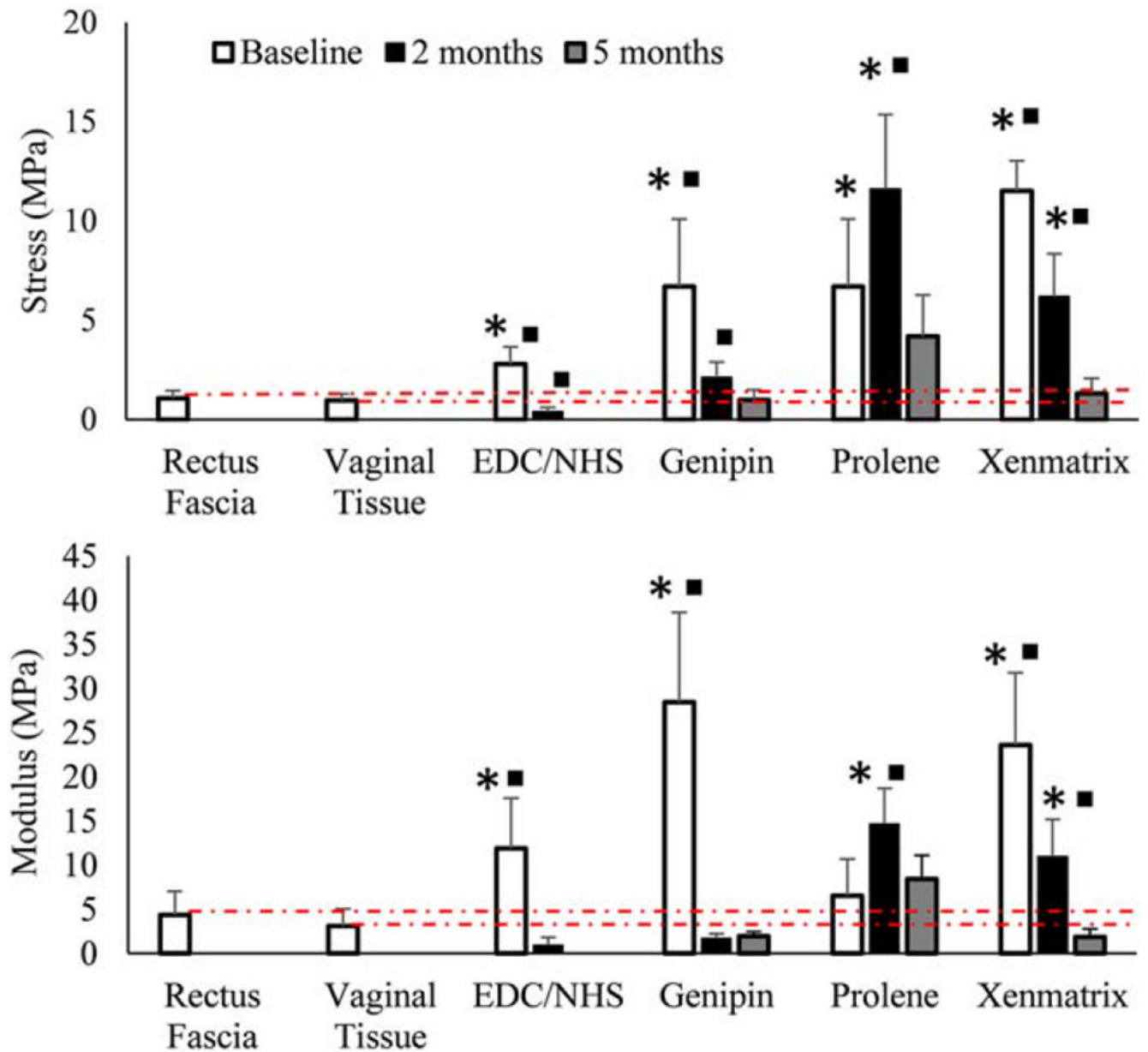
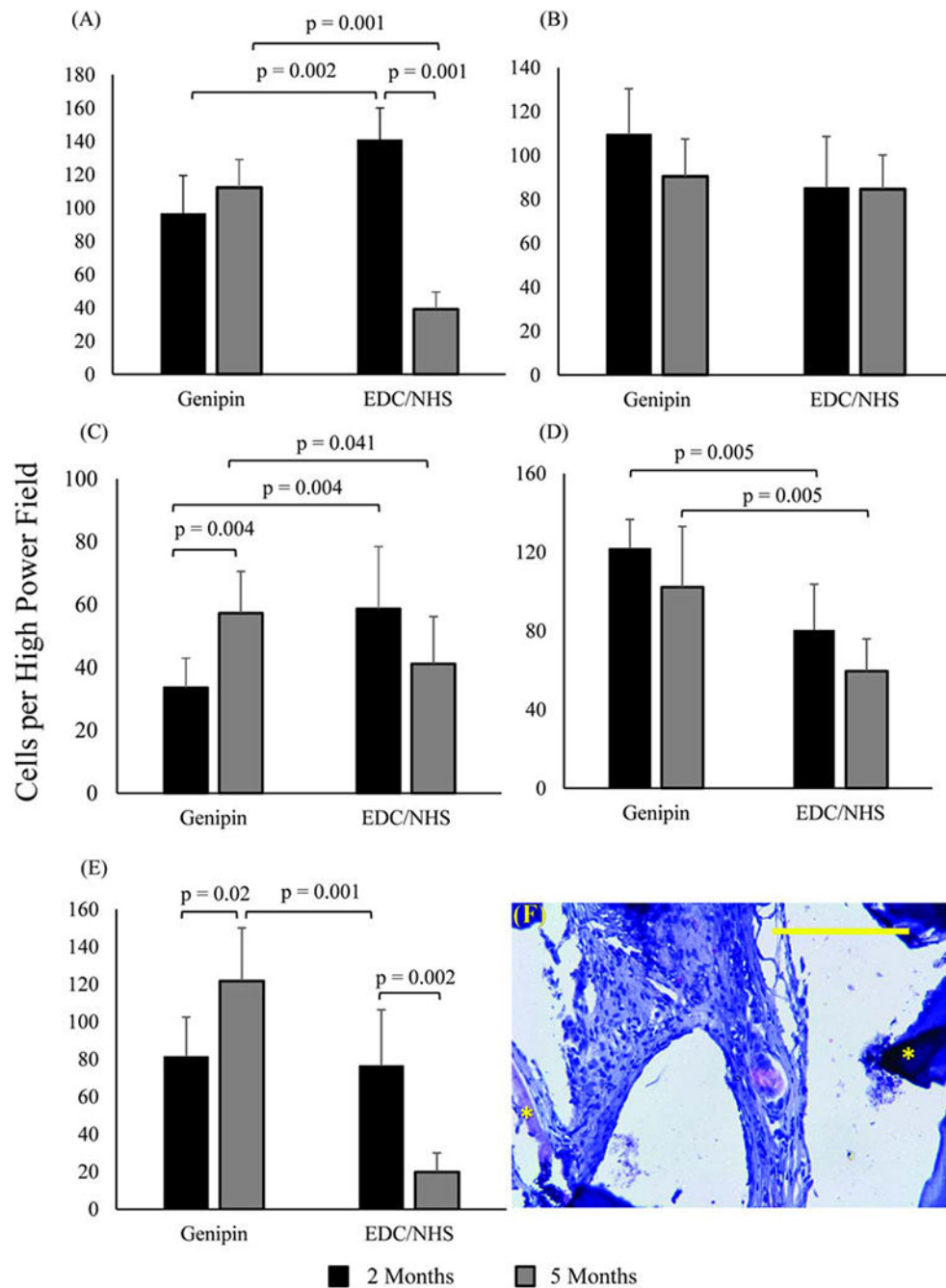


FIGURE 4.

Average (A) modulus and (B) stress to failure for meshes over time ($n = 5$ per time point). Squares indicate a value is significantly different ($p < 0.05$) from the preceding value (intra-group comparison) and stars indicate that a given value is significantly different ($p < 0.05$) from native tissue at that time point (inter-group comparison). Dashed red lines are meant to show how meshes compare to native tissues over time. Error bars indicate the SD for test groups.

**FIGURE 5.**

Immunohistochemical identification of macrophage markers in woven collagen scaffolds. (A) General macrophage marker CD68, (B) pro-inflammatory macrophage markers B7, and (C) IL6, anti-inflammatory macrophage markers (D) CD163, and (E) CD206. In all bar graphs $n = 15$ per time point and horizontal connecting bars indicate a significant difference ($p < 0.05$) between the number of expressive cells for groups. Error bars indicate the SD for test groups (F) Immunohistochemical image of CD206 positive macrophages in genipin crosslinked collagen meshes. Asterisks highlight collagen threads. The scale bar is 0.25 mm.

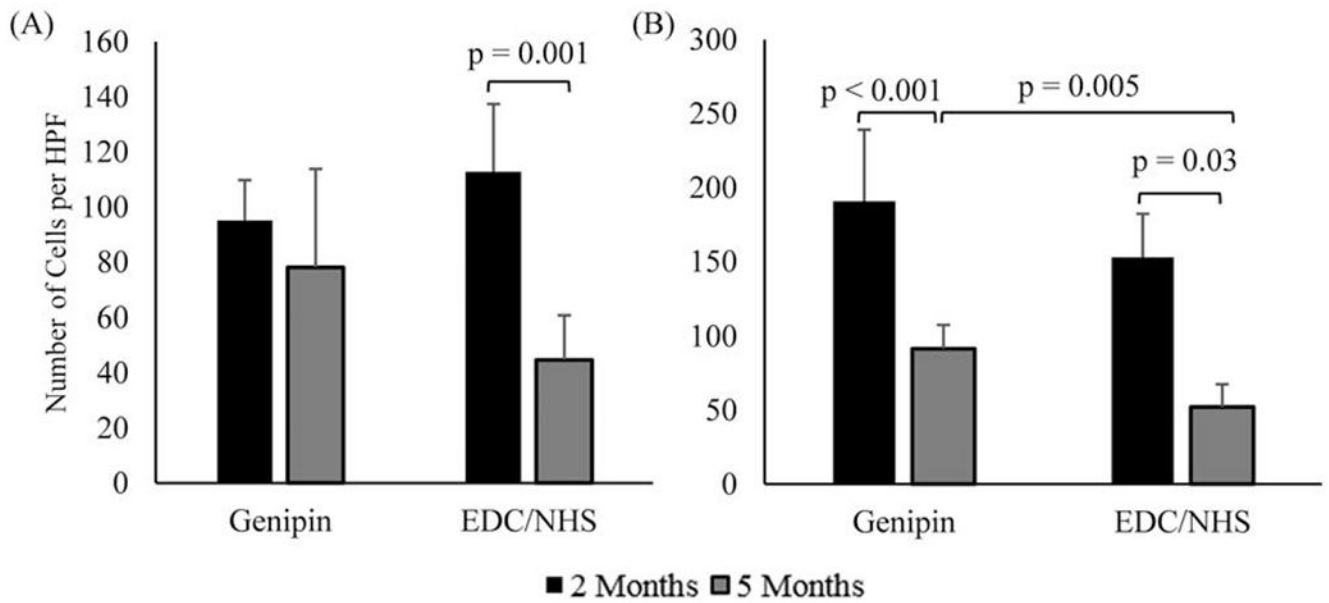
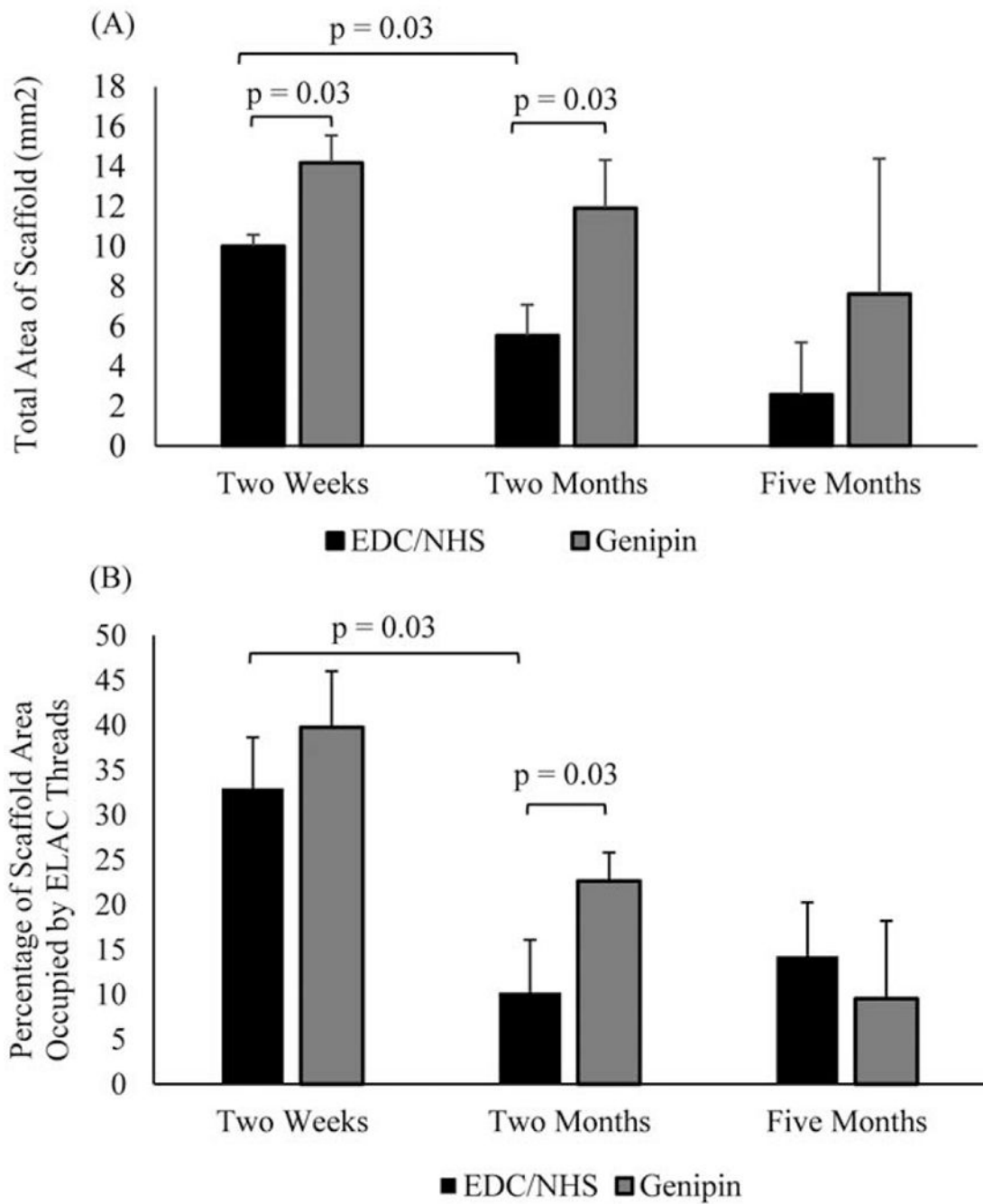


FIGURE 6.

Immunohistochemical markers for endothelium in woven collagen meshes at 2 and 5 months ($n = 15$ per time point). (A) CD31 and (B) α -SMA. Horizontal connecting bars indicate a significant difference ($p < 0.05$) between the number of expressive cells for groups, and error bars indicate the SD for test groups.

**FIGURE 7.**

Changes in the (A) morphology and (B) thread area density of woven collagen scaffolds over time. Significant differences are indicated by connecting bars ($p < 0.05$) and error bars indicate the SD for test groups.

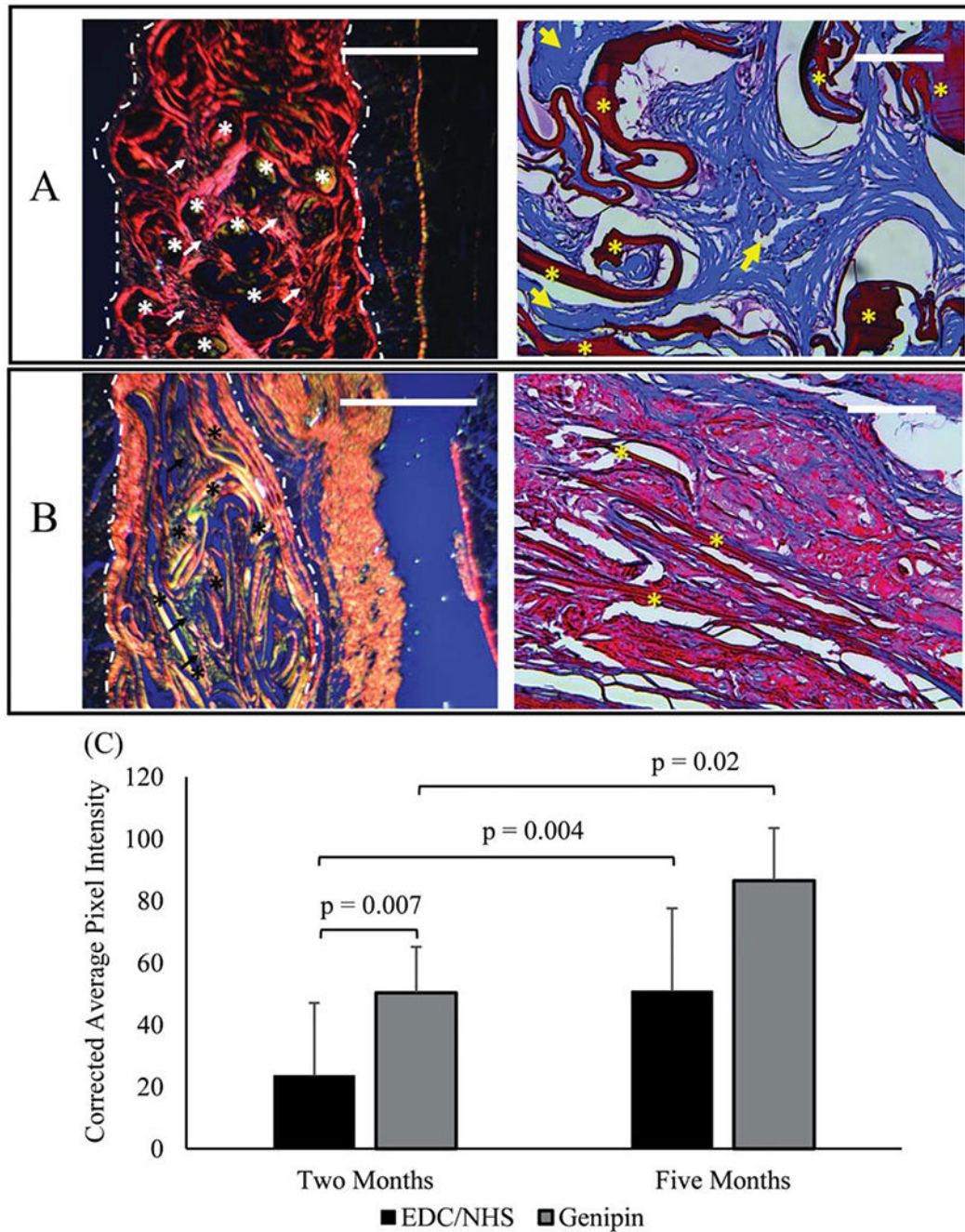


FIGURE 8.

Five months explanted GCC (A) and ECC (B) meshes stained using picosirius red (left) and Masson's trichrome (right). Picosirius red stained slides were imaged under cross polarized conditions. Highly aligned collagen is predominant in GCC samples as manifested by red/orange polarization patterns and loosely aligned collagen is predominant in ECC as manifested by yellow/green polarization in picosirius stained sections. Masson's trichrome images show ample amount of de novo collagen deposition (arrows) in genipin crosslinked threads (asterisk). On the other hand, there is minimal collagen deposition in EDC/NHS

crosslinked threads. (C) Degree of alignment of newly deposited collagen from picrosirius stained sections was measured by the corrected pixel intensity of images of scaffolds at 2 and 5 months ($n = 15$ per time point). Significant differences are indicated by connecting bars ($p < 0.05$), and error bars indicate SD for test groups. Scale bars for picrosirius and Masson's trichrome images are 1 mm and 0.25 mm in length, respectively.

TABLE I.

Host Response Evaluation^{a,b}

	Granulation Tissue		Foreign Body Reaction		Fibrous Encapsulation			
	2 weeks	2 months	2 weeks	2 months	2 weeks	2 months	5 months	
EDC/NHS	2 ± 0.82	4 ± 0	2 ± 0	3.25 ± 0.96	4 ± 0	4 ± 0	2 ± 0	2 ± 0
Genipin	2.25 ± 0.96	2.8 ± 0.84	1 ± 0	3.75 ± 0.5	3 ± 0	3.67 ± 0.58	2.5 ± 0.58	4 ± 0
Prolene	1 ± 0	0.8 ± 0.45	1 ± 0	2 ± 0	2 ± 0	2 ± 0	3 ± 0	3.2 ± 0.45
Xenmatrix	0.25 ± 0.5	0 ± 0	0 ± 0	2.5 ± 0.58	2 ± 0	2 ± 0	3 ± 0	4 ± 0

^aParameters were defined as follows: granulation tissue: a precursor to fibrous tissue formation, indicated by the presence of macrophages, blood vessels and fibroblasts; foreign body response: indicated by the presence of foreign body giant cells, macrophages and monocytes; fibrous encapsulation: indicated by the presence of acellular collagen around the perimeter of mesh materials. Acute and chronic inflammation scores were zero for all but two ECC meshes (one at 2 weeks and one at 2 months); thus, inflammation scores are not included in the table

^bScoring for host response parameters reported as the mean ± SD of scores at 2 weeks, 2 months and 5 months. Scores were given on a scale from 0 to 4; 0 = no presence of host response characteristic, 1 = minimal presence, 2 = mild presence, 3 = moderate presence and 4 = extensive presence. Parameters were measured at the perimeter of mesh materials. *N* = 5 slides were scored in total for each parameter for each mesh type at each time point, or 1 slide per explanted sample from each animal at each time point.

TABLE II.

Tissue Integration^{a,b}

	Neovascularization			Cellular Infiltration			Collagen Deposition			Fibroblast Proliferation		
	2 weeks	2 months	5 months	2 weeks	2 months	5 months	2 weeks	2 months	5 months	2 weeks	2 months	5 months
EDC/NHS	1.25 ± 0.4	1.2 ± 0.4	2 ± 0	4 ± 0	3.75 ± 0.4	4 ± 0	1.5 ± 0.5	2.2 ± 0.4	2 ± 1 [*]	1.5 ± 0.5	2.2 ± 0.4	2 ± 1
Genipin	2.75 ± 0.4	1.2 ± 0.4	2.33 ± 0.5	3.5 ± 0.5	3.2 ± 0.4	4 ± 0	2 ± 0	2.8 ± 0.4	3.5 ± 0.5 [*]	2 ± 0	2.8 ± 0.4	3.5 ± 0.5
Prolene	1 ± 0	0.6 ± 0.8	2 ± 0	1 ± 0	1 ± 0.6	4 ± 0	3.67 ± 0.5	2.2 ± 0.45	3.75 ± 0.5 [*]	3.67 ± 0.47	2.2 ± 0.4	2.75 ± 0.82
Xenmatrix	0 ± 0	0 ± 0	0 ± 0	0 ± 0	0 ± 0	0 ± 0	0 ± 0	0 ± 0	0 ± 0	0 ± 0	0 ± 0	0 ± 0

^{*} Mann-Whitney pair-wise tests for new collagen deposition scores run between Prolene and GCC and Prolene and ECC meshes showed no significant differences.

^a Parameters were defined as follows: neovascularization: indicated by the presence and outgrowth of capillary buds and sprouts; cellular infiltration: indicated by the density of nuclei within the bulk of the scaffold material; new collagen deposition: indicated by cellularized area with quasi aligned collagen fibers conforming to the direction of the mesh material; fibroblast proliferation: indicated by the density of fibroblasts within the bulk of the mesh material.

^b Scoring for tissue integration parameters reported as the mean ± SD at 2 weeks, 2 months and 5 months. Scores were given on a scale from 0 to 4; 0 = no presence of tissue integration characteristic, 1 = minimal presence, 2 = mild presence, 3 = moderate presence and 4 = extensive presence. Parameters were measured within mesh materials. *N* = 5 slides were scored in total for each parameter for each mesh type at each time point, or 1 slide per explanted sample from each animal at each time point.

TABLE III.

Results of Mechanical Testing of Baseline and Recovered Meshes^a

Sample Type		Failure Stress (MPa)	Young's Modulus (MPa)
Genipin	Baseline	6.7 ± 3.4*■	24.8 ± 10.1*■
	2 weeks	2.1 ± 0.8■	1.7 ± 0.5
	5 months	1.0 ± 0.5	3.6 ± 2.9
EDC/NHS	Baseline	2.8 ± 0.9*■	11.9 ± 5.9*■
	2 weeks	0.4 ± 0.2■	1.0 ± 0.9
	5 months	N/A	N/A
Prolene	Baseline	6.7 ± 3.4*	7.6 ± 3.5
	2 weeks	11.6 ± 3.8*■	14.7 ± 4.0*■
	5 months	4.2 ± 2.1	8.4 ± 2.7
Xenmatrix	Baseline	11.5 ± 1.5*■	23.6 ± 8.2*■
	2 weeks	6.2 ± 2.2*■	11.0 ± 4.2*■
	5 months	1.3 ± 0.8	1.9 ± 1.0
Rectus Fascia	Baseline	1.1 ± 0.4	4.4 ± 2.7
Vaginal tissue	Baseline	1.0 ± 0.3	3.1 ± 1.9

^aValues are reported as mean ± SD with values from baseline, 2 months and 5 months time points listed in descending order in each cell. Squares indicate a value is significantly different from the proceeding value (intra-group comparison) and stars indicate that a given value is significantly different from native tissue at that time point (inter-group comparison). EDC/NHS meshes could not be collected for mechanical testing at 5 months. As such, all values have been replaced with N/A.